Membrane and Water Treatment, *Vol. 14, No. 3 (2023) 129-140*
https://doi.org/10.12989/mwt.2023.14.3.129

Experimental and model study on the mixing effect of injection method in UV/H_2O_2 process

Heekyong Oh*[1], Pyonghwa Jang[2], Jinseok Hyung[1], Jayong Koo[1] and SungKyu Maeng[3]

[1]*Department of Environmental Engineering, University of Seoul, 163 Seoulsiripdaero, Dongdaemun-gu, Seoul 02504, Republic of Korea*
[2]*R&D Center, OCI, R&D Center, OCI, 61 Sagimakgol-ro 62beon-gil, Jungwon-gu, Seongnam-si, Gyeonggi-do, 13212, Republic of Korea*
[3]*Department of Civil and Environmental Engineering, Sejong University, 209 Neungdong-ro, Gwangjin-gu, Seoul 05006, Republic of Korea*

(Received May 31, 2023, Revised August 8, 2023, Accepted August 23, 2023)

Abstract. The appropriate injection of H_2O_2 is essential to produce hydroxyl radicals (OH·) by mixing H_2O_2 quickly and exposing the resulting H_2O_2 solution to UV irradiation. This study focused on evaluating mixing device of H_2O_2 as a design factor of UV/H_2O_2 AOP pilot plant using a surface water. The experimental investigation involved both experimental and model-based analyses to evaluate the mixing effect of different devices available for the H_2O_2 injection of a tubular hollow pipe, elliptical type of inline mixer, and nozzle-type injection mixer. Computational fluid dynamics analysis was employed to model and simulate the mixing devices. The results showed that the elliptical type of inline mixer showed the highest uniformity of 95%, followed by the nozzle mixer with 83%, and the hollow pipe with only 18%, after passing through each mixing device. These results indicated that the elliptical type of inline mixer was the most effective in mixing H_2O_2 in a bulk. Regarding the pressure drops between the inlet and outlet of pipe, the elliptical-type inline mixer exhibited the highest pressure drop of 15.8 kPa, which was unfavorable for operation. On the other hand, the nozzle mixer and hollow pipe showed similar pressure drops of 0.4 kPa and 0.3 kPa, respectively. Experimental study showed that the elliptical type of inline and nozzle-type injection mixers worked well for low concentration (less than 5mg/L) of H_2O_2 injection within 10% of the input value, indicating that both mixers were appropriate for required H_2O_2 concentration and mixing intensity of UV/ H_2O_2 AOP process. Additionally, the elliptical-type inline mixer proved to be more stable than the nozzle-type injection mixer when dealing with highly concentrated pollutants entering the UV/H_2O_2 AOP process. It is recommended to use a suitable mixing device to meet the desired range of H_2O_2 concentration in AOP process.
Keywords: AOP; CFD UV/ H_2O_2; inline mixer; mixing; nozzle mixer; uniformity

1. Introduction

Chemical injection devices are used in water treatment facilities for various processes such as coagulation, oxidation, AOP (advanced oxidation process), and disinfection. These devices are used to remove impurities such as turbidity, colloidal particles, dissolved organic and inorganic matters, and inactivate pathogenic micro-organisms from water (Lin *et al*. 2013, Byun *et al*. 2005, Jang *et al*. 2021, Lee *et al*. 2023, Mysore *et al*. 2004). Commonly chemicals used in water treatment plants include liquid chemicals like coagulants, flocculant aids, pH adjusters, hydrogen peroxide, and chlorine as well as gaseous chemicals such as ozone and solid substances like powdered activated carbon. The injection devices should have the capability to quickly and accurately inject the appropriate amount of chemicals over a wide range in response to changes in flow rate and water quality load entering the reactor, and they should have the ability to mix with the target raw water quickly entering the reactor. Additionally, they should facilitate rapid mixing with the target water after the predetermined amount has been injected to the bulk (KWWA 2023).

There are two methods of injecting liquid chemicals into the reactor of a water treatment plant: surface drop injection and internal pressure injection. The selection of the mixing method connected to the injection device depends on the characteristics of the chemical, agitation speed, mixing time, and required reaction mechanism. The injection point for chemicals varies based on the mixing method and can be the surface drop point, the area near the agitator blade, or the center of the inflow pipe, where rapid mixing can occur during injection (Craik *et al*. 2003, McConnachie *et al*. 1999).

The purpose of rapid mixing in chemical injection is to ensure even dispersion of the chemical in a short period. Rapid mixing is crucial when using metal salt coagulants like alum or ferric chloride because these coagulants disperse within seconds and instantly adsorb to colloidal particles (Chan *et al*. 2017). However, for chemicals such as chlorine, alkaline solutions, ozone, and potassium permanganate, which do not undergo hydrolysis, it is more important to have sufficient reaction time with contact time through rapid mixing (Vadasarukkai *et al.* 2015).

The injection concentration of chemicals used in water treatment plants involves a liquid-liquid mixing process. However, unlike general industrial plant processes, a very small amount of chemicals, with a water-to-chemical ratio of 1:50,000 to 1:200,000, must be instantly supplied to the raw water and diffused. This requires precise control of low

*Corresponding author, Professor,
E-mail: heekyong.oh@uos.ac.kr

http://www.techno-press.org/?journal=mwt&subpage=7
ISSN: 2005-8624 (Print), 2092-7037 (Online)

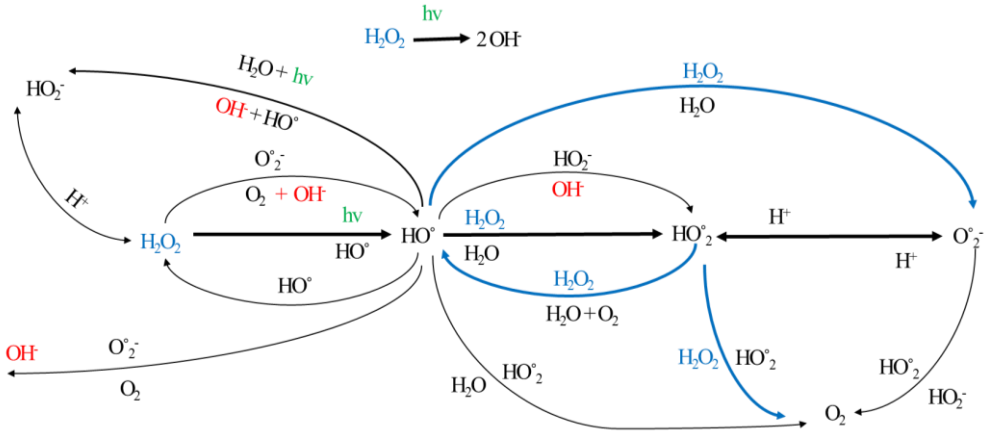

Fig. 1 Reaction pathway of the UV/H_2O_2 process without reaction with background compounds

injection amounts. Inline fixed mixing devices offer the advantage of not requiring external power during chemical injection and can be applied in the field where a loss of head is secured without a separate contact point (Lei *et al.* 2022, Oh and Lee, 2005). In recent years, their applicability has been widely reviewed as they can secure mixing time within seconds inside the pipe (Thakur *et al.* 2003, Hosseini *et al.* 2019, Chan *et al.* 2017, Singh *et al.* 2009).

Recently, as the water quality of water resources has deteriorated due to climate change and urbanization, taste and odor causing compounds, toxins, saturated hydrocarbons, 1-4 dioxane, pharmaceuticals, disinfection by-products and emerging pollutants such as perfluorinated compounds, are detected at high frequencies and concentration, causing problems. These compounds are generally removed through oxidation, advanced oxidation processes (AOP), adsorption, NF, and RO processes (Fedorov *et al.* 2022, Shahid *et al.* 2021, Marcoux *et al.* 2017, Hübner *et al.* 2015, Zhang *et al.* 2013, Feng *et al.* 2012, Bottino *et al.* 2011). AOP processes are employed to oxidatively remove non-degradable organic matter, to improve biodegradability by generating a powerful oxidant, hydroxyl radical (OH·), through the combination of oxidizing agents such as ozone, chlorine, and ultraviolet light or pH adjustment (Miklos *et al.* 2018, Carmen *et al.* 2018, Ike *et al.* 2019).

In other words, the AOP process using ozone as an oxidizing agent (oxidation-reduction potential, 2.07 eV) generate OH· with a higher oxidation-reduction potential of 2.8 eV by combining with other substances like high pH, hydrogen peroxide, ultraviolet light, titanium dioxide, electron beams, and metal oxides to oxidize the bio-degradable organic matter (Seo *et al.* 2019, Zeng *et al.* 2020). However, ozone-based AOP processes have certain drawbacks, including reduced efficiency of activated carbon adsorption due to residual dissolved ozone after the reaction, the creation of hazardous working environments due to atmospheric ozone gas, and the requirement of large-scale contactors for the oxidation reaction (Kwon *et al.* 2015, Park *et al.* 2019). To overcome these drawbacks of ozone-based AOP processes, hydrogen peroxide (H_2O_2)-based ultraviolet (UV) processes can be used as an alternative (Tian *et al.* 2020, Heydari *et al.* 2021, Ye *et al.* 2021).

H_2O_2 has the characteristic of being odorless compared to other oxidants and does not generate reaction byproducts in aqueous solutions. It can be utilized over a wide range of pH values. UV radiation generates ultraviolet radiation at wavelengths below 230nm, which enhances the efficiency of water treatment and facilitates the conversion of oxygen into ozone. Fig. 1 shows reaction pathway of the UV/H_2O_2 process for the degradation of the parent compound, without considering the background compounds (Rubio-Clemente *et al.* 2017).

UV/H_2O_2 process initiates the primary photolysis H_2O_2 or HO_2-, producing HO^0. When H_2O_2 is dissolved in water, it produces the conjugate base HO_2-, which acts as an initiator for decomposing ozone more quickly than OH·. Consequently, OH· generated through various pathways reacts non-selectively with dissolved organic matter in a short period of time. Furthermore, recombination of HO^0 can occur to produce H_2O_2. However, free radicals can react with H_2O_2 and HO_2- and producing HO_2^0 when the oxidant is in excess. HO_2^0 is less reactive than HO^0, but can degrade organics with a high amount of radicals in the pathways. It can produce O_2^{0-}, which, can participate in degradation and mineralization. Therefore, in the UV/H_2O_2 process, the efficient generation of OH· is achieved by rapidly mixing and dissociating H_2O_2 and exposing the resulting solution to UV irradiation (Rosenfeldt and Linden 2007).

When hydrogen peroxide is used in the UV/H_2O_2 AOP process, the appropriate amount of injection and mixing depends on the type and concentration of the target contaminant (Jang *et al.* 2021). Insufficient or excessive injection of H_2O_2, as well as inadequate mixing with the influent, can have downstream impacts on processes such as GAC treatment. For instance, insufficient H_2O_2 injection or poor mixing in the AOP process can lead to rapid breakthrough of activated carbon due to the influent of undecomposed contaminants. In the case of polymer contaminants, they may not be adequately adsorbed and could be discharged into the effluent. On the other hand, excessive injection of H_2O_2 can oxidize the solid activated carbon itself, causing carbon particle collapse and discharge into the effluent.

In this study, experiments were conducted on a pilot-scale plant of 100m^3/day installed in a reservoir to determine

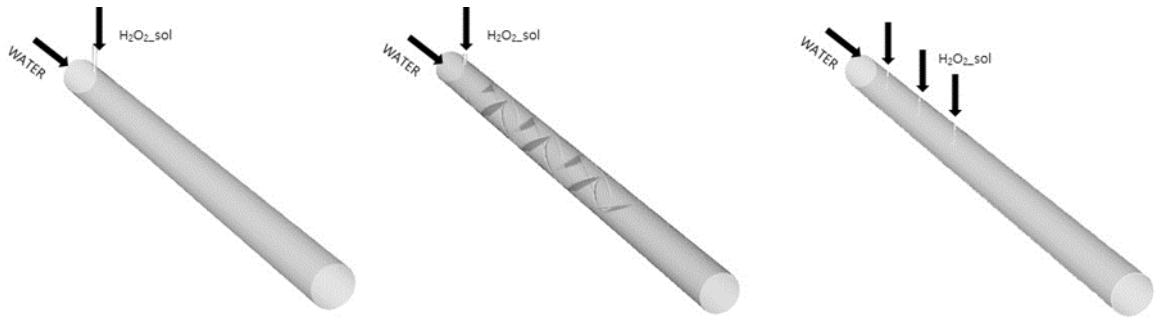

(a) Hollow pipe (b)Elliptical typed in-line mixer (c)Nozzle mixer

Fig. 2 CFD domains of various mixers tested in this study

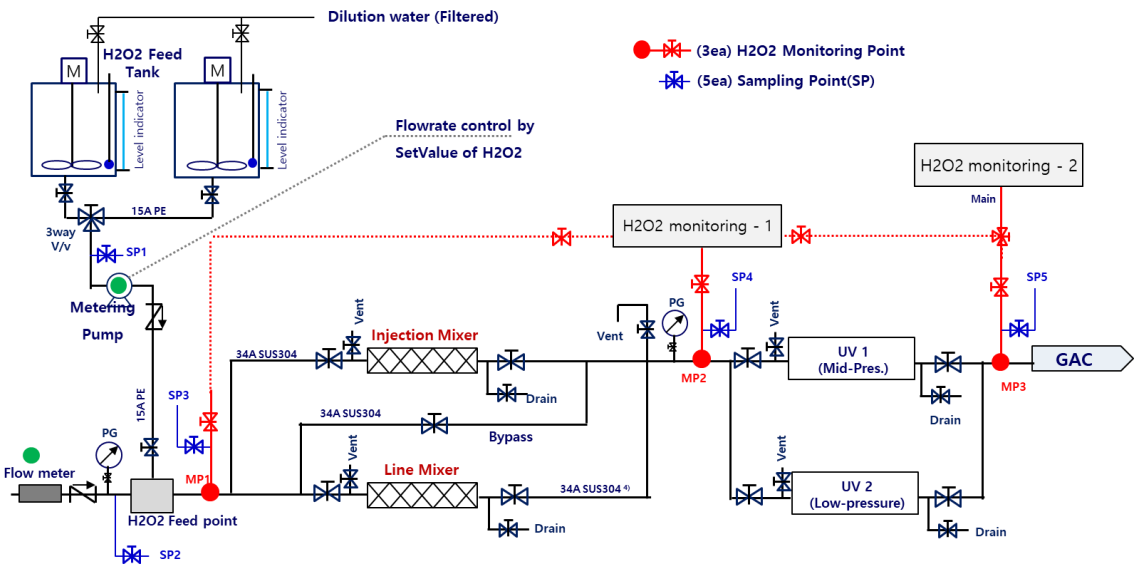

Fig. 3 Outline of UV/ H_2O_2 AOP process

the proper injection device of H_2O_2 in the UV/H_2O_2 AOP process. Two types of chemical injection devices, namely nozzle type and inline mixer type, were compared and evaluated for their mixing effect to analyze the H_2O_2 dissolution characteristics. The primary focus was on the online measurement of the injection concentration of H_2O_2 and the residual H_2O_2 with respect to the mixing devices. Additionally, computational fluid dynamics (CFD) were used to analyze the mixing characteristics and uniformity of the three types of mixed devices, allowing for a comprehensive understanding of the experimental results. These experimental results, along with the CFD data, serve as guidelines for the analysis of various H_2O_2 injection devices, aiding in the selection of a suitable device to optimize the UV/ H_2O_2 AOP process.

2. Materials and method

2.1 Design of mixing apparatus and binary property

Three types of hydrogen peroxide mixing devices that can be used in a UV/ H_2O_2 AOP pilot-scale process to mix 5% hydrogen peroxide solution and AOP influent (membrane-treated water) were considered. The first H_2O_2 solution mixing device was based on a structure that connected H_2O_2 inlet pipe of 5mm diameter to a main pipe with diameter of 32 mm (Fig. 2) and distance 610 mm from discharge point to injection point of H_2O_2 solution was secured for the injection conditions of the raw water and H_2O_2 solution to ensure numerical stability (Fig. 7(a)). The other two mixing devices were built by selecting a static mixer (line mixer) and injection nozzle mixer that are commonly used as in-pipe mixing devices.

2.2 UV/H_2O_2 AOP pilot plant

The UV/ H_2O_2 AOP pilot plant had a processing capacity of 100 m^3/day, and the process configuration was shown in Fig. 3, while the actual picture of plant was shown in Fig. 4. The AOP process was combined with coagulation and 0.1μm membrane filtration as pretreatment processes. The raw water was a surface water. The AOP facility consisted of H_2O_2 injection and mixing equipment, H_2O_2 storage tank, H_2O_2 concentration monitoring device (Q46/84 Hydrogen Peroxide Monitor, ATi company), and UV oxidation device (WEDECO Spectro 50e, Evoqua). Experiments were performed to evaluate the optimal usage

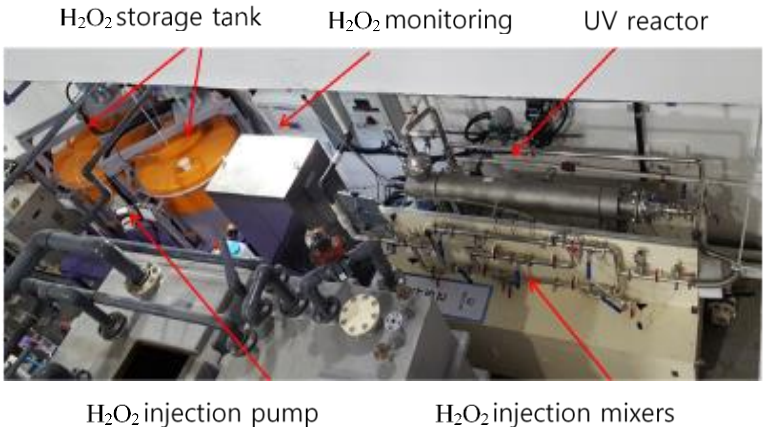

Fig. 4 UV/ H_2O_2 AOP pilot plant used for test bed

Table 1 Values of the parameters I and POW_{cr} for some popular membranes for water permeation

Solutions	Flow rate	Weight load (kg/s)	MW(g/mol)	Density[1)] (kg/m^3)	Viscosity[1)] (kg/m.s)
H2O2	12.20 ml/min	2.08E-04	34.0147	1021.36	0.0008895
Water	100 m^3/d	1.15532	18.0152	998.2	0.0009125

1) At 15℃, density and viscosity for hydrogen peroxide and water from ASPEN+ database

and residual concentration of H_2O_2 in the AOP process. The H_2O_2 monitoring device measured the injection concentration and residual concentration after the UV reactor to identify the mixing effect of mixer type. The injection concentration was controlled by injecting a 5% H_2O_2 solution into the influent (filtered water). Two types of mixing devices, a line mixer and an injection mixer, were installed and compared through experimental testing.

The chemical feed pump was designed to maintain hydrogen peroxide concentration between 0~20 mg/L, following injection and mixing in the process. The tank stored 5% hydrogen peroxide, with a storage period of 30 days, to facilitate a controlled feed of 20 mg/L hydrogen peroxide concentration within the AOP process. To ensure proper dilution of the product, stainless steel agitators were installed within the tanks, preventing any reactivity with hydrogen peroxide. Additionally, level gauges were equipped on the tanks, providing external measurement of residual hydrogen peroxide capacity, while vent holes were installed in the tank lids to allow for the safe discharge of trace amounts of oxygen gas that may be generated during hydrogen peroxide decomposition.

For the hydrogen peroxide transfer metering pumps, peristaltic pumps were used to minimize contact with hydrogen peroxide. The pumps used were able to prevent reverse flow due to water pressure during hydrogen peroxide injection and could fine-tune the flow rate, allowing for the production of hydrogen peroxide concentrations within the target range of 0-20 mg/L in the AOP process. To monitor changes in hydrogen peroxide concentration in real-time during UV/ H_2O_2 AOP process, two hydrogen peroxide concentration monitoring devices were installed at three monitoring points: before and after the mixer unit to measure the initial and mixed hydrogen of H_2O_2, removal efficiency of taste and odour compounds, peroxide concentration, respectively, and after the UV unit to measure the hydrogen peroxide concentration after the UV treatment. Samples collected from each monitoring point could be measured using either of the two monitoring devices by switching the valve. Based on a pilot plant raw water capacity of 100 m^3/d, the supply flow rate for a 5% hydrogen peroxide solution to achieve a hydrogen peroxide concentration of 10 mg/L was calculated (Table 1). For an accurate comparison of interpretations, it is desirable to interpret simulation results based on the same residence distance criteria. Therefore, in this study, the concentration distribution of hydrogen peroxide solution was compared and evaluated based on a cross-section 610 mm after the hydrogen peroxide solution injection point. A symmetric scheme was used to calculate the interphase intersection area. Other physical properties of the fluid were used for simulation in the binary property H_2O_2 solution and water based on Schiller-Naumann equation of drag coefficient and Schiller-Naumann equation of interfacial area, 2.88E-05 of mass diffusivity(m^2/s), 0.5 of virtual mass coefficient.

The Table 2 shows the hydrogen peroxide injection conditions for evaluating the performance of the H_2O_2 injection mixer. The starting material for the UV/H_2O_2 AOP process cannot easily change the hydrogen peroxide concentration in the hydrogen peroxide storage tank. Therefore, the injection flow rate was varied using a transfer pump to induce changes in the hydrogen peroxide concentration within the process while maintaining the injection hydrogen peroxide concentration at 5%.

2.3 CFD based mixing effect analysis of H_2O_2 injection system

The numerical analysis of the hydrogen peroxide injection and mixing was performed using commercial

software ANSYS FLUENT 18.0, which utilizes the finite volume method based on the inspection volume. FLUENT is a universal CFD code that can be applied to the entire fluid range, from incompressible to supersonic flow, and allows users to achieve accurate and efficient flow analysis. It is also a software that can be used to analyze various physical phenomena such as turbulent flow, unsteady state analysis, heat transfer analysis, chemical reaction flow, and multiphase flow (Haddadi *et al* 2020, Rahmani *et al* 2007, Rauline *et al* 2000). To prevent excessive numerical diffusion during the analysis process of the mixing device, the High-Resolution Interface Capturing (HRIC) scheme and Green-Gauss Node-based (GGN) scheme were applied. HRIC adopted in this study helps accuracy and stability. Depending on the calculation method for gradients and derivatives, it affects the results of the advection and the diffusion term in the flow conservation equation. GGN has the advantages of more accuracy and minimize false diffusion.

The symmetry scheme was used to calculate the interfacial boundary area. In addition, the simulation utilized the physical properties of the fluid based on values obtained through the mixing-law. The numerical analysis was performed using the coupled algorithm under steady-state assumption, without considering the energy. The simulation focused on the raw water and a 5% hydrogen peroxide solution. The concentration distribution of hydrogen peroxide solution was compared and evaluated based on a cross-section located 610mm downstream from the hydrogen peroxide injection point. This interpretation allowed for the examination of simulation results at the same residence distance. In this study, the coupled algorithm was used to perform a coupled analysis of pressure and velocity, and the general dependent variable values at the grid interface for momentum and turbulence were calculated using a second-order upwind scheme. The conservation equations of mass and momentum, known as the Navier-Stokes equations, were interpreted in the tensor coordinates system as shown in Eq. (1).

For mass conservation:

$$\frac{\partial \rho}{\partial t} + \nabla \cdot (\rho \vec{v}) = S_m \tag{1}$$

where, S_m is the mass source from dispersed second phase and to be added to the continuous phase.

For conservation momentum:

$$\frac{\partial}{\partial t}(\rho \vec{v}) + \nabla \cdot (\rho \vec{v}\vec{v}) = -\nabla \mathrm{P} + \nabla \cdot \bar{\bar{\tau}} + \rho \vec{g} + \vec{P} \tag{2}$$

where, $\bar{\bar{\tau}}$ is stress tensor, $\vec{v}$ is Absolute fluid velocity component, P is static pressure, $\rho \vec{g}$ is gravitational body force and , $\vec{P}$ is external body forces.

Regarding turbulent flow, other dependent variables can be considered as overall average values. In this study, an eddy viscosity model was applied, which focuses on molecular gradient-diffusion and turbulent motion. The k-ε model, consisting of transport equations for turbulence kinetic energy (k) and its dissipation rate (ε), was adopted. To improve excessive wall modeling in the k-ε model, the ε transport equation was improved and the scalable wall function technique was applied to the near-wall region in the Realized k-ε model. The water and H_2O_2 solution investigated in this study are miscible substances, so the Eulerian model was used among the multiphase models. The Eulerian model solves the following mass conservation equation for a single phase, which can be seen as a continuum:

Table 2 Hydrogen peroxide concentration range to be tested

Parameters	Case 1	Case 2	Case 3
UV/H_2O_2 target concentration (Calculated, %)	65	4	2
Flow rate of influent (m3/hr)		4.2	
Concentration of H_2O_2 (measured, %)		5.1	
Flow rate of H_2O_2 (ml/min)	85	5.5	2.8
Injection dose of H_2O_2 (calculated, mg/L)	65	4.0	2.0

$$\frac{\partial}{\partial t}(\alpha_q \rho_q) + \nabla \cdot (\alpha_q \rho_q \vec{v}) = \sum_{p=1}^{n} (\dot{m}_{pq} - \dot{m}_{qp}) + S_q \tag{3}$$

$$f = \frac{C_D Re}{24} \tag{4}$$

$$\mathrm{C}_D = \begin{cases} \dfrac{24(1 + 0.15Re^{0.687})}{Re} & Re \le 1000 \\ 0.44 & Re > 1000 \end{cases} \tag{5}$$

The distribution and mixing between target substances was determined based on the qualification of species mixing, individually. Therefore, the degree of mixing of the target component was determined as 'uniformity', which is calculated by the volume fraction efficiency of the target at the cross-section, and the closer to 1 means a uniform distribution.

$$\text{Uniformity} = 1 - \frac{\sum_{i=1}^{N}\left[\sqrt{(x_i - \bar{x})^2} A_i\right]}{2\bar{x}\mathrm{A}} \tag{6}$$

where, A *is* surface area, where A_i *is* surface area at the i-th cell, x_i is variable (fraction or concentration) at the i-th cell, and $\bar{x}$ is the area-weighted variable of surface.

3. Results and discussions

3.1 Evaluation of mixing effect using hollow pipe

The hollow pipe type was selected as the control group for the mixing device, which hydrogen peroxide solution was injected from the top into an empty cylindrical tube through which the raw water flows. Although it has a Reynolds number of 4.43×10^4, which indicates turbulent flow in terms of calculation, the internal flow of the tube is almost laminar and can be confirmed through Path line (Fig. 5). The analysis of the volume fraction of H_2O_2 inside the hollow pipe showed that H_2O_2 mixing throughout the entire interior of the hollow pipe was not sufficient, as shown in

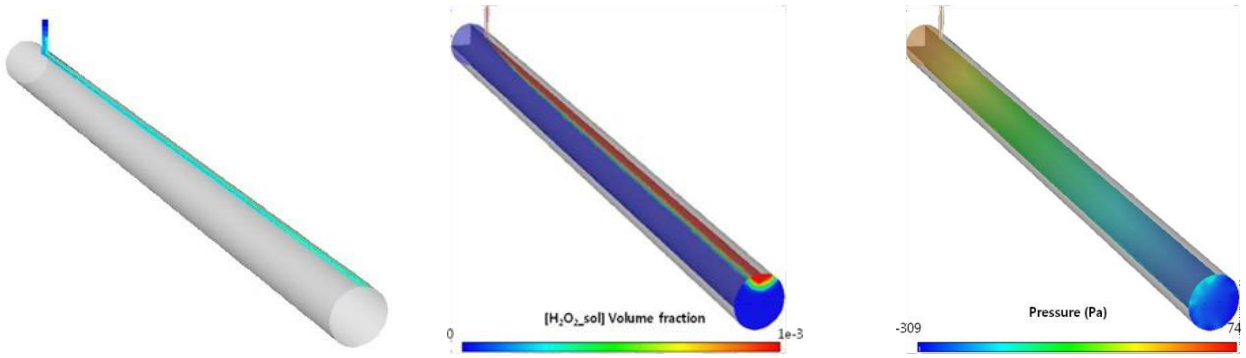

(a)Path line of H_2O_2 sol (b)Volume fraction contour of H_2O_2 sol (c)Pressure drop contour of H_2O_2 sol

Fig. 5 Volume fraction and pressure drop of H_2O_2 solution in hollow pipe

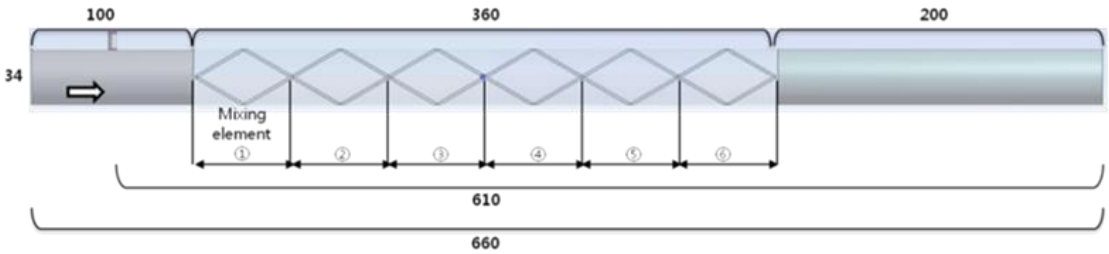

(a) CFD domain of elliptical-type inline mixer

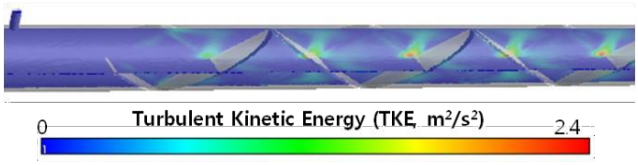

(b) Turbulent KE contour

Fig. 6 Turbulent KE contour in elliptical-type inline mixer

Fig. 5(b). A significant portion of the area where H_2O_2 solution does not reach was observed at the outlet of the pipe, and the uniformity at the outlet was calculated by 18.2%. For H_2O_2 injection pipe, there was no structure inside the pipe, so only pressure drop occurred due to friction on the stainless steel pipe wall as shown in Fig. 5(b). The analysis showed that the pressure drop from the raw water inlet to the outlet was calculated as ΔP 285 (Pa), which was in good agreement with the calculated value of the Darcy-Weisbach equation (287.6 Pa). The values in the initial and end of the contour were minimum and maximum, which differed from the average value of the inlet and outlet of the pipe when calculating delta pressure.

3.2 Evaluation of mixing effect using elliptical-type inline mixer

As an inline mixer, multiple elements were typically inserted into the pipe to induce mixing in the fluid flow. In this study, an elliptical-type inline mixer was designed and applied to a 34mm diameter pipe. Each semi-elliptical element was fixed inside the injection pipe in a staggered arrangement. Each element was assumed to fill the inner diameter of the pipe completely after the H_2O_2 injection point. The inlet diameters for the water and hydrogen peroxide solution were set to 34mm and 5mm, respectively, as shown in Fig.6(a). The total length of the structure zone of the elliptical-type inline mixer was 360mm, and the point after the additional 200mm was taken as a standard so that it was not affected by the geometry structure thereafter. The diluted H_2O_2 was injected at 50mm before the inner elliptical-type structure of the inline mixer, the concentration distribution at the 610mm distance (50mm + 360mm + 200mm) point after injection was analyzed. The nozzle injection case was compared based on the point after the same retention distance of 610mm after the diluted H_2O_2 was injected for comparison with the case of the elliptical-type inline mixer. As shown in Fig. 6(b), CFD examined the velocity profile inside the inline mixer pipe and calculated the average flow velocity of the water by 1.2 m/s. However, the fluid was dispersed radially along each elliptical-type element, converged, and then divided into two, repeating the process of merging and generating turbulence due to the deformation of the fluid flow caused by the elliptical elements.

The repetition of strong and weak patterns of flow rates through each element was also related to the development of the preceding turbulence. Since water and H_2O_2 were miscible fluids, the flow after mixing was almost the same (Figs. 7(a) and (b)). Through the vector, it was possible to observe the repeated behavior of the stream converging and diverging up and down to the left and right. As shown in Figs. 7(c) and (d), the residence time of the water and H_2O_2 solution increased as they passed through each element of

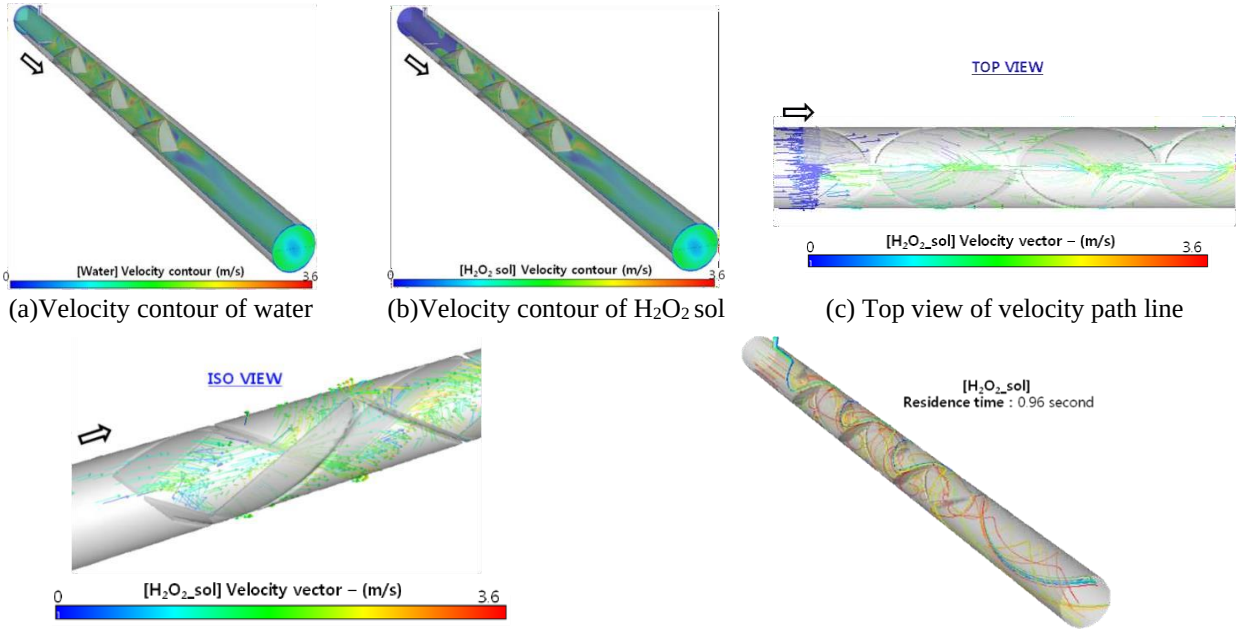

(a)Velocity contour of water (b)Velocity contour of H_2O_2 sol (c) Top view of velocity path line

(d) Iso view of velocity path line (e) Velocity vector of H_2O_2 solution

Fig. 7 Velocity contour of water and H_2O_2 solution in elliptical-type inline mixer

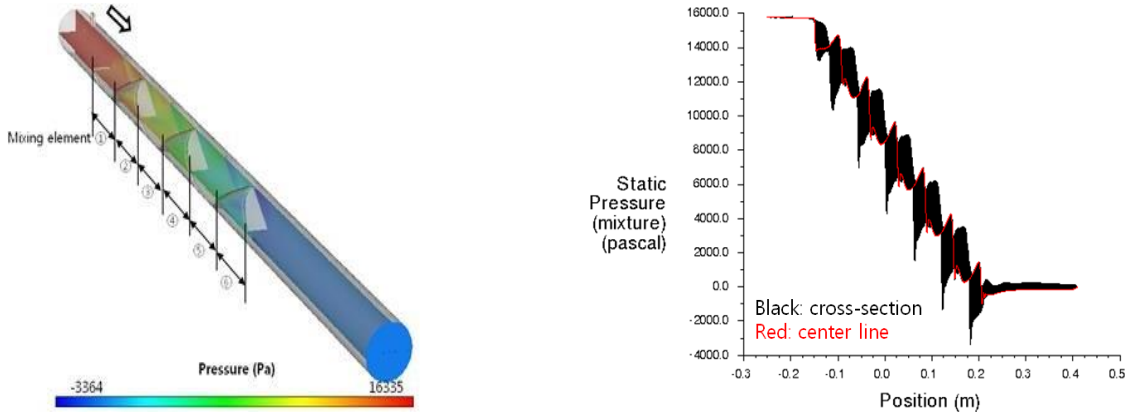

(a) Pressure contour (b) Pressure plot at each position

Fig. 8 Pressure contour and pressure plot in elliptical-type inline mixer

the pipe. The entire piping system, including the inline mixer, had a residence time of 0.96 seconds, increasing the mixing efficiency Fig. 7(e).

As the water and H_2O_2 solution pass through each element of the piping, pressure drops occurred. As shown in Fig. 8(a) and (b), a pressure drop of approximately 2,500 Pa was observed for each element, and the pressure drop at the inlet and outlet was 15,775 Pa. When compared to the calculated value (15 kPa) for an inline mixer with five elements of the same type and diameter from another company's mixing device, a very similar value was observed.

The uniformity value of H_2O_2 solution at the outlet was calculated to be 94.5%, and the volume fraction of H_2O_2 solution at the outlet was nearly uniform. It could be confirmed that a certain level of uniform mixing had already been achieved at the fifth element of the piping (Fig. 9)

3.3 Evaluation of mixing effect using nozzle injection mixer

Nozzle mixer was applied using the principle of spraying small particles through a narrow hole. The L-shaped nozzle with a diameter of 0.5 mm was designed to inject hydrogen peroxide solution into the center of the pipe. The pipe diameter was 34 mm, and three nozzles were positioned at 110 mm intervals to face the opposite direction of the water flow (Fig. 10(a)). In addition, three nozzles were installed but only the nozzle at the very front was used to inject H_2O_2 solution. The flow conditions were the same as in case 0 and case 1. Turbulence was induced by placing the nozzle in the opposite direction to the main flow, but it was difficult to effectively induce turbulence due to the nozzle in the manner as shown in Fig. 10(b) due to the very small injection capacity compared to the injection diameter of H_2O_2 solution. The flow direction and

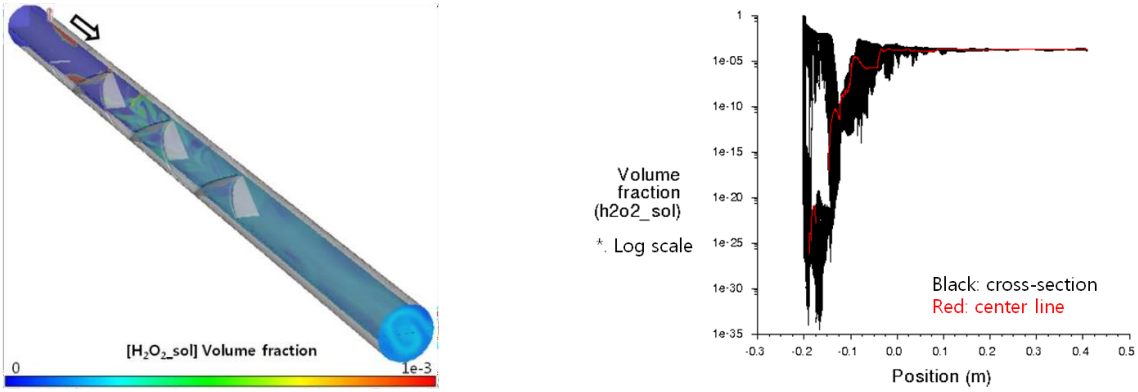

(a) Volume fraction contour (b) Volume fraction plot at each position

Fig. 9 Volume fraction contour and plot in elliptical-type inline mixer

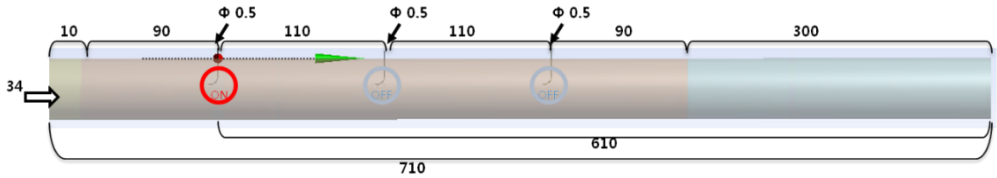

(a) CFD domain of nozzle mixer

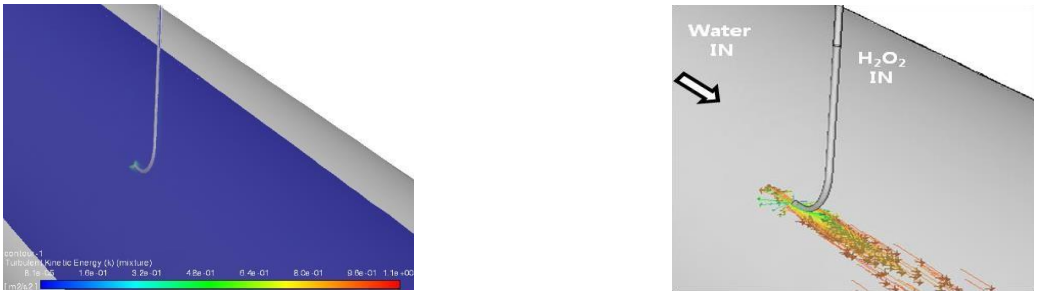

(b) Turbulent KE contour (c)Velocity vector

Fig. 10 Turbulent KE contour and velocity vector of H_2O_2solution in nozzle mixer

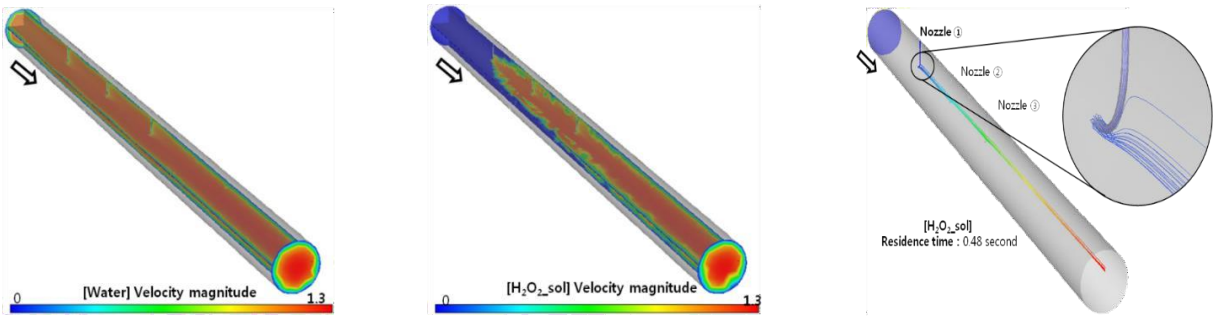

(a)Water solution H_2O_2 solution (c) Path line

Fig. 11 Velocity contour and path line of H_2O_2 in nozzle mixer

driving force could be seen through the velocity vector, and it was confirmed that the velocity in the reverse direction was almost negligible (Fig. 10(c)).

The average flow rate inside the pipe is 1.1~1.2 m/s and even with the application of nozzles, the maximum flow rate is limited to 1.29 m/s, which could explain these results. The flow inside the pipe can be considered almost uniform in velocity with respect to the incoming water. As shown in Fig. 11, it eventually flowed towards the outlet through the flow of water, although the hydrogen peroxide solution was injected in the opposite direction of the water flow from the nozzle. The residence time increased by counter-flow injection against the flow of the raw water, but it only lasted for 0.48 seconds. This was half the value compared to the elliptical-type inline mixer.

On the other hand, the nozzle mixer structure has no elements other than the nozzle that hinder the flow in the pipeline, so it is advantageous under pressure. The pressure

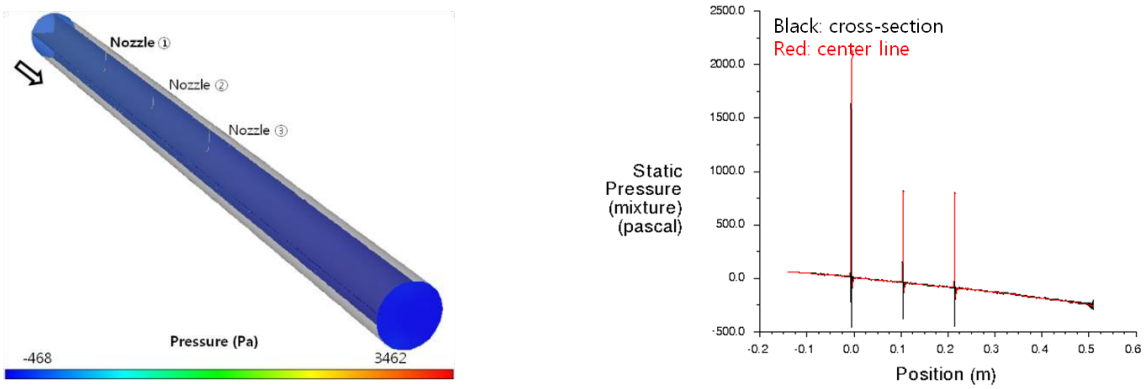

(a) Pressure contour (b) Pressure plot at the distance

Fig. 12 Pressure contour and Plot in Nozzle mixer

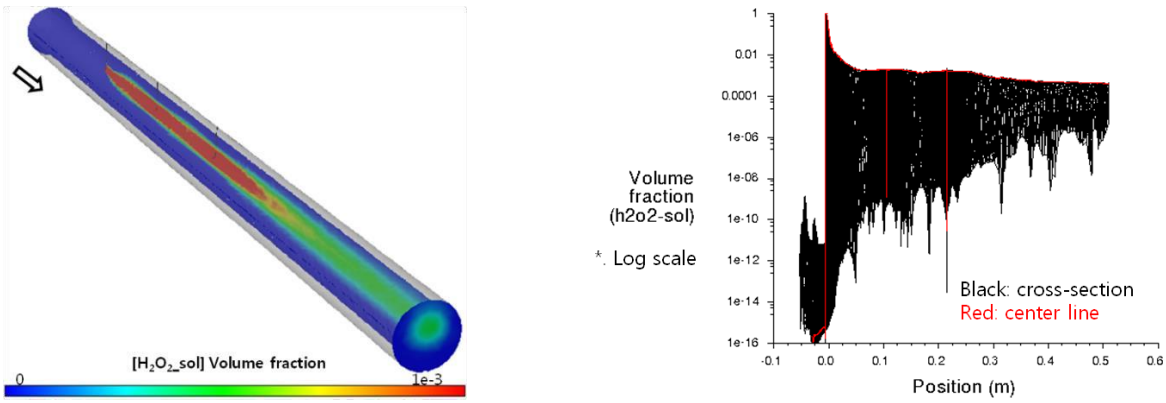

(a) Volume fraction contour (b) Volume fraction plot

Fig. 13 Volume fraction contour and Plot of H_2O_2 solution in nozzle mixer

drop between the inlet and outlet was calculated to be 360 Pa calculated through CFD, which was almost the same level as that of a hollow pipe (Fig. 12)

Hydrogen peroxide solution introduced into the pipe through the nozzle was gradually mixed with raw water and discharged. A weak turbulence was generated by wall friction on the surfaces of the three spray nozzles as shown below, and the hydrogen peroxide solution diffused into a concentric form with a slight upward center relative to the center cross section of the pipe. After the injection of hydrogen peroxide, most were distributed around the center of the pipe. These results yielded a uniformity of approximately 83.10%, which was not superior to the elliptical inline mixer, but to the lowest structural component was considered to have better mixing performance than the hollow pipe (Fig. 13).

3.4 Comparison of mixing effect and uniformity using different mixers

The feasibility of applying a static mixer to H_2O_2 solution mixing in a UV/H_2O_2 AOP pilot plant was examined, and several experiments were conducted to investigate the necessary technical aspects for improving the mixing efficiency. The uniformity of H_2O_2 solution distribution inside the pipe and pressure drop for three different cases of mixing pipes were summarized in Table 3. The uniformity of H_2O_2 solution distribution in the pipeline was initially at a level of 1.5% just after injection, but after passing through each mixing device in each case, the elliptical-type inline mixer showed a high uniformity of 95%, whereas the nozzle mixer showed 83%, and the hollow pipe only showed 18%. When comparing the pressure drops, the elliptical-type inline mixer showed the highest pressure drop of 15.8 kPa, which was unfavorable for operation. The nozzle mixer and hollow pipe showed similar pressure drops of 0.4 kPa and 0.3 kPa, respectively.

3.5 Experimental evaluation of H_2O_2 injection mixers in AOP pilot plant

The influent of the UV/ H_2O_2 AOP process was membrane filtrate with a turbidity of 0.05 NTU or less and a DOC of 2.5±0.2 mg/L. The dose of hydrogen peroxide in the AOP process was determined by the operating concentration range of 2 to 5 mg/L based on DOC removal when combined with UV irradiation. The goal of the pilot test was to evaluate whether the determined hydrogen peroxide concentration value could be mixed after injection and maintained prior to UV irradiation. Both injection doses were tested by 2 and 4 mg/L of H_2O_2 and H_2O_2 concentration was monitored at the outlet of mixer after

Table 3 Simulation results of uniformity and pressure drop

Type	Uniformity		Pressure drop(ΔP)
	at the inlet	at the outlet	
Hollow pipe	1.5 %	18.2 %	0.29 kPa
Elliptical-type inline mixer	1.4 %	94.5 %	15.78 kPa
Nozzle-type injection mixer	1.5 %	83.1 %	0.36 kPa

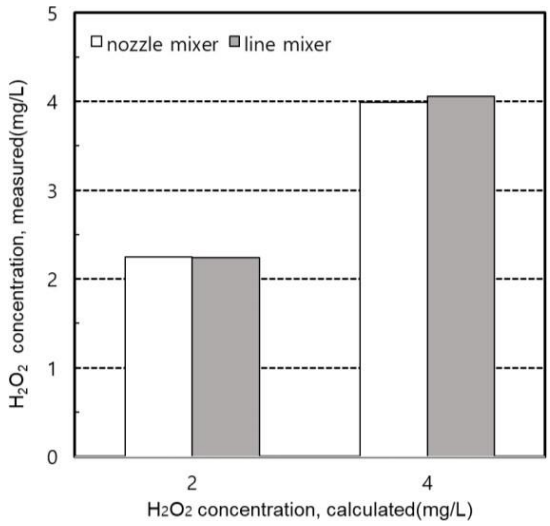

Fig. 14 Measured concentration of H_2O_2 using different mixer at low concentration

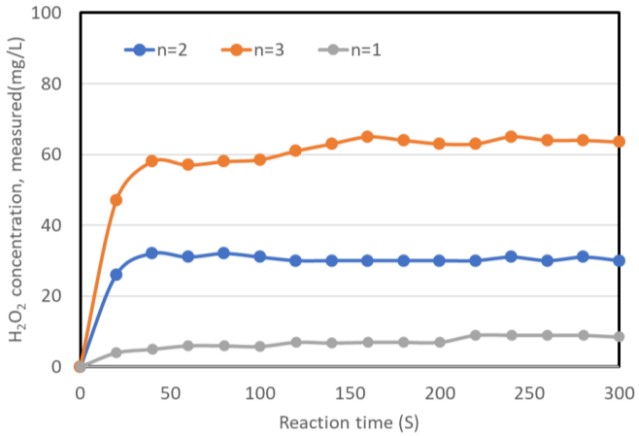

(a)Measured H_2O_2 with nozzle

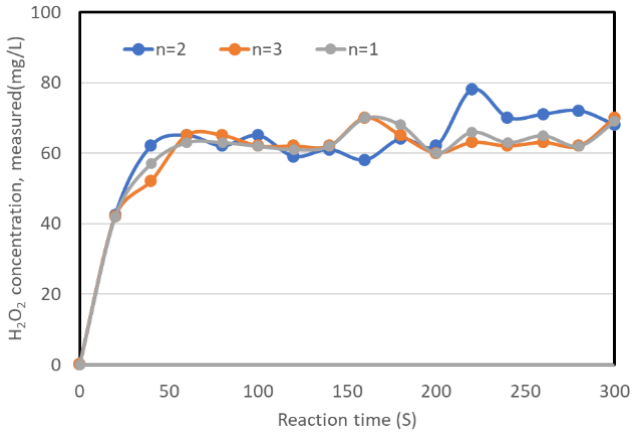

(b)Measured H_2O_2 with line mixer

Fig. 15 Measured concentration of H_2O_2 using different mixer at high concentration

injection. It was impossible to measure the hydrogen peroxide concentration profile via contact time of minute, such as the rapid mixing through CFD study. As a result, the H_2O_2 concentration was measured several times for one day at the outlet of the mixer. The injection condition of 2 mg/L exhibited a slightly larger deviation from the calculated value compared to the 4 mg/L of injection condition as shown in Fig. 14. Nevertheless, it was confirmed that both types of mixers provided stable H_2O_2 injection mixing, with an average deviation within 10% of the calculated values.

To compare the performance of the H_2O_2 injection mixers, the H_2O_2 concentration was adjusted to 60 mg/L, and measurements were taken at 20-second intervals at the end of both types of mixed teeth. For the nozzle-type injection mixer, only one of the experimental results reached the same concentration as the injection condition, with all three trials eventually converging to a constant concentration, taking approximately 140 seconds. On the other hand, for the inline mixer, the concentration of the injection condition converged within 60 seconds in all rounds, but some concentration deviation occurred. The nozzle-type injection mixer with a small injection diameter of 0.5 mm faced issues with lowering static pressure in the injection pipe, leading to an increase in friction loss and a smaller amount of H_2O_2 being injected into the mixing device. Conversely, the elliptical-type inline mixer with a larger diameter of 5.0 mm had no problems with the amount of H_2O_2 injection. However, it showed slight discrepancies from the CFD result condition due to dynamic fluid flow changes, resulting in slightly lower mixing time and mixing power compared to the CFD result (Fig. 15). The results of the high-concentration hydrogen peroxide injection experiment showed that the inline mixer could operate more stably in terms of injection mixing compared to the nozzle mixer.

4. Conclusions

This study focused on optimizing one part among the design factors of the UV/H_2O_2 AOP pilot process in a water intake facility using a reservoir. The goal was to efficiently produce hydroxyl radicals (OH·) by mixing H_2O_2 quickly and exposing the resulting H_2O_2 solution to UV irradiation. The study evaluated the mixing characteristics of different devices used for the H_2O_2 injection using a tubular hollow pipe, elliptical-type in-line mixer, and nozzle-type injection mixer.

Computational Fluid Dynamics (CFD) analysis was employed to model and simulate the mixing devices. The results showed that the initial uniformity of H_2O_2 solution distribution in the pipeline right after injection was 1.5%. but after passing through each mixing device, the elliptical-type in-line mixer demonstrated the highest uniformity of 95%, followed by the nozzle mixer with 83%, and the hollow pipe with only 18%. This indicated that the elliptical-

type in-line mixer was the most effective. Regarding pressure drops, the elliptical-type in-line mixer exhibited the highest pressure drop of 15.8 kPa, which was unfavorable for operation. On the other hand, the nozzle mixer and hollow pipe showed similar pressure drops of 0.4 kPa and 0.3 kPa, respectively. Experimental study showed that the elliptical-type in-line and nozzle-type injection mixers worked well for low concentration (less than 5mg/L) of H_2O_2 injection within 10% of the input value, indicating that both mixers were appropriate for required H_2O_2 concentration and mixing intensity of UV/ H_2O_2 AOP process. Additionally, the elliptical-type in-line mixer proved to be more stable than the nozzle-type injection mixer when dealing with highly concentrated pollutants entering the UV/H_2O_2 AOP process. Uniformity and H_2O_2 concentration measurement were used to evaluate the mixing effect of H_2O_2, further studies will be conducted on the optimization of UV/H_2O_2 AOP through various changes in individual mixers and OH radical analysis.

Acknowledgments

This work was supported by the Korean Ministry of Environment as the "Global Top Project (RE201606104). This work was supported by the 2022 Research Fund of the University of Seoul (202204081003).

References

Bottino, A., Capannelli, G., Comite, A., Ferrari F. and Firpo, R. (2011), "Water purification from pesticides by spiral wound nanofiltration membrane", *Membr. Water treat.*, **2**(1), 63-74. https://doi.org/10.12989/mwt.2011.2.1.063.

Byun, S., Oh, J., Lee, B. and Lee, S. (2005), "Improvement of coagulation efficiency using instantaneous flash mixer (IFM) for water treatment", *Colloid. Surface. A.*, **268**(1-3), 104-110. https://doi.org/10.1016/j.colsurfa.2005.06.027.

Carmen, T., Gilca, A.F., Barjoveanu, G. and Fiore, S. (2018), "Emerging pollutants removal through advanced drinking water treatment: A review on processes and environmental performances assessment", *J. Clean. Prod.*, **197**, 1210-1221. https://doi.org/10.1016/j.jclepro.2018.06.247.

Chan, S.N., Qiao, Q.S., Lee, J.H.W., Choi, K.W. and Huang, J.C. (2017), "Modeling of mixing and rapid chlorine demand in sewage disinfection with dense chlorine jets", *J. Environ. Eng.*, **143**(11), 04017074. https://doi.org/10.1061/(ASCE)EE.1943-7870.000127.

Craik, S.A., Smith, D.W., Chandrakanth, M. and Belosevic, M. (2003), "Effect of turbulent gas–liquid contact in a static mixer on Cryptosporidium parvum oocyst inactivation by ozone", *Water Res.*, **37**(15), 3622-3631. https://doi.org/10.1016/S0043-1354(03)00285-9.

Fedorov, K., Dinesh, K., Sun, X., Soltani, R.D.C, Wang, Z., Sonawane, S. and Boczkaj G. (2022), "Synergistic effects of hybrid advanced oxidation processes (AOPs) based on hydro-dynamic cavitation phenomenon–A review", *Chem. Eng. J.*, **432**, 134191. https://doi.org/10.1016/j.cej.2021.134191.

Feng. C.Y., Matsuura, T., Ismail, A.F. (2012), "Progresses in membrane and advanced oxidation processes for water treatment", *Membr. Water Treat.*, **3**(3), 181-200. https://doi.org/10.12989/mwt.2012.3.3.181.

Haddadi, M.M., Hosseini, S.H., Rashtchian, D. and Olazar, M. (2020), "Comparative analysis of different static mixers performance by CFD technique: An innovative mixer", *Chinese J. Chem. Eng.*, **28**(3), 672-684. https://doi.org/10.1016/j.cjche.2019.09.004.

Heydari, F., Osfouri, S., Abbasi, M., Dianat, M.J., Khodaveisi, J. (2021), "Treatment of highly polluted grey waters using Fenton, UV/ H2O2 and UV/TiO2 processes", *Membr. Water treat.*, **12**(3), 125-132. https://doi.org/10.12989/mwt.2021.12.3.125.

Hosseini, S.M., Razzaghi, K. and Shahraki, F. (2019), "Design and characterization of a Low-pressure-drop static mixer", *AlChE J.*, **65**(3), 1126-1133. https://doi.org/10.1002/aic.16505.

Hübner, U., von Gunten, U. and Jekel, M. (2015), "Evaluation of the persistence of transformation products from ozonation of trace organic compounds-A critical review", *Water Res.*, **68**, 150-170. https://doi.org/10.1016/j.watres.2014.09.051.

Ike, I.A., Karanfil, T., Cho, J.W. and Hur, J. (2019), "Oxidation byproducts from the degradation of dissolved organic matter by advanced oxidation processes-a critical review", *Water Res.*, **164**, 114929. https://doi.org/10.1016/j.watres.2019.114929.

Jang, P., Kim, H., Kyung, G. and Oh, H. (2021), "Improved mixing of hydrogen peroxide injection in advanced oxidation process treatment using computational fluid dynamics", *Desalin. Water. Treat.*, **227**, 124-131. http://doi.org/10.5004/dwt.2021.27359.

Kwon, M., Kim, S., Ahn, Y., Jung, Y., Joe, W.H., Lee, K. and Kang, J. (2015), "Removal of residual ozone in drinking water treatment using hydrogen peroxide and sodium thiosulfate", *J. Korean Soc. Water Wastewater*, **29**(4), 481-491. https://doi.org/10.11001/jksww.2015.29.4.481.

KWWA (Korea Water and Wastewater Works Association. (2023), "Injection facility of coagulation", in: Design standards of water supply system(commentary), Korean Ministry of Environment, 678-693.

Lee, J.H.W., Qiao, Q.S., Chan, S.N., Choi, K.W. and Chau, H.K.M. (2023), "Reduction of chlorine disinfection dosage through optimal jet design in the Hong Kong harbor area treatment scheme", *J. Environ. Eng.*, **149**(2), 05022009. https://doi.org/10.1016/JOEEDU.EEENG-6868.

Lei, H., Guan, X., Sun, Y. and Yan, H. (2022), "A novel design of in-line static mixer for permanganate/bisulfite process: Numerical simulations and pilot-scale testing", *Water Environ. Res.*, **94**(5), e10725. https://doi.org/10.1002/wer.10725.

Lin, J.L., Pan, J.R. and Huang, C. (2013), "Enhanced particle destabilization and aggregation by flash-mixing coagulation for drinking water treatment", *Sep. Purif. Technol.*, **115**, 145-151. https://doi.org/10.1016/j.seppur.2013.05.013.

Marcoux, A., Pelletier, G., Legay, L., Bouchard, C. and Rodriguez, M.J. (2017), "Behavior of non-regulated disinfection by-products in water following multiple chlorination points during treatment", *Sci. Total Environ.*, **586**, 870-878. https://doi.org/ 10.1016/j.scitotenv.2017.02.066.

McConnachie, G.L., Folkard, G.K., Mtawali, M.A. and Sutherland, J.P. (1999), "Field trials of appropriate hydraulic flocculation processes", *Water Res.*, **33**(6), 1425-1434. https://doi.org/10.1016/S0043-1354(98)00339-X.

Miklos, D.B., Remy, C., Jekel, M., Linden, K.G., Drewes, J.E. and Hübner, U. (2018), "Evaluation of advanced oxidation processes for water and wastewater treatment–A critical review", *Water Res.*, **139**, 118-131. https://doi.org/10.1016/j.watres.2018.03.042.

Mysore, C., Leparc, J., Lake, R., Agutter, P. and Prévost, M. (2004), "Comparing static mixer performances at pilot and full scale for ozonation, inactivation of bacillus subtilis, and bromate formation in water treatment", *Ozone Sci. Eng.*, **26**(2), 207-215. https://doi.org/10.1080/01919510490439609.

Oh, J.I. and Lee, S.H. (2005), "Influence of streaming potential on flux decline of microfiltration with in-line rapid pre-coagulation

process for drinking water production", *J. Membrane Sci*., **254**(1-2), 39-47. https://doi.org/10.1016/j.memsci.2004.12.030.

Park, J.I., Lee, Y., Jang, K.A, Kim, T.H., Park, C.J. and Yoo, J.H. (2019), "A study on the optimization about peroxone(O3/H2O2 -AOP)-quenching process in G water treatment plant for 2-MIB treatment and residual ozone removal", *J. Korean Soc. Environ. Eng*., **41**(12), 703-715. https://doi.org/10.4494/KSEE.2019.41.12.703.

Rahmani, R.K., Ayasoufi, A. and Keith, T.G. (2007), "A numerical study of the global performance of two static mixers", *J. Fluid. Eng*., **129**(3), 338-349. https://doi.org/10.1115/1. 2427082.

Rauline, D., Le Blévec, J.M., Bousquet, J. and Tanguy, P.A. (2000), "A comparative assessment of the performance of the Kenics and SMX static mixers", *Chem. Eng. Res. Des*., **78**(3), 389-396. https://doi.org/10.1205/026387600527284.

Rubio-Clemente, A., Chica, E. and Peñuela, G.A. (2017) "Kinetic modeling of the UV/ H2O2 process: determining the effective hydroxyl radical concentration", *in Physico-Chemical Wastewater Treatment and Resource Recovery*, Intech. https://doi.org/10.5772/67803.

Seo, J.W., Jeong, J.Y., Lee C.H. (2019), "Photocatalytic degradation of organic compounds by 2-ethyimidazole-treated titania under visible light lumination", *Membr. Water treat*., **10**(3), 223-229. https://doi.org/10.12989/mwt.2019.10.3.223.

Shahid, M.K., Kashif, A., Fuwad, A. and Choi, Y. (2021), "Current advances in treatment technologies for removal of emerging contaminants from water–A critical review", *Coordin. Chem. Rev*., **442**, 213993. https://doi.org/10.1016/j.ccr.2021.213993.

Singh, M.K., Kang, T.G., Anderson, P.D., Meijer, H.E.H. and Hrymak, A.N. (2009), "Analysis and optimization of low-pressure drop static mixers", *AlChE J*., **55**(9), 2208-2216. https://doi.org/10.1002/aic.11846.

Thakur, R.K., Vial, C., Nigam, K.D.P., Nauman, E.B. and Djelveh, G. (2003), "Static mixers in the process industries-A review", *Chem. Eng. Res. Des*., **81**(7), 787-826. https://doi.org/10.1205/026387603322302968.

Tian, F., Ye, W., Xu, B., Hu, X., Ma, S., Lai, F., Gao, Y., Xing, H., Xia, W. and Wang, B. (2020), "Comparison of UV-induced AOPs(UV/Cl2, UV/NH2Cl, UV/ClO2 and UV/H2O2) in the degradation of iopamidol: Kinetics, energy requirements and DBPS-related toxicity in sequential disinfection processes", *Chem. Eng. J*., **398**, 125570. https://doi.org/10.1016/j.cej.2020.125570.

Vadasarukkai, Y.S. and Gagnon, G.A. (2015), "Application of low-mixing energy input for the coagulation process", *Water Res*., **84**, 333-341. https://doi.org/10.1016/j.watres.2015.07.049.

Ye, C., Ma, X., Deng, J., Li, X., Li, Q. and Dietrich, A. M. (2021), "Degradation of saccharin by UV/H2O2 and UV/PS processes: A comparative study", *Chemosphere*, **288**, 132337. https://doi.org/10.1016/j.chemosphere.2021.132337.

Zeng, H., Zhang, G., Ji, Q., Liu, H., Hua, X., Xia, H., Sillanpää, M. and Qu, J. (2020), "pH-independent production of hydroxyl radical from atomic H*- mediated electrocatalytic H2O2 reduction: A green fenton process without byproducts", *Environ. Sci. Technol*., **54**, 14725-14831. https://doi.org/10.1021/acs.est.0c04694

Zhang, J., Sun, B. and Guan, X. (2013), "Oxidative removal of bisphenol a by permanganate: Kinetics, pathways and influences of co-existing chemicals", *Sep. Purif. Technol*., **107**, 48-53. https://doi.org/10.1016/j.seppur.2013. 01.023.